

# Investigation on Degradation Process of PdRuIr/CZ “pseudo-Rh” Catalysts used for Motorcycles

Takuya Motegi Shunya Tataru Shunpei Takamoto Kosuke Doi

当論文は、JSAE 20249016/SAE 2024-32-0016として、SETC2024 (Small Powertrains and Energy Systems Technology Conference)にて発表されたものです。

Reprinted with permission Copyright © 2024 SAE Japan and Copyright © 2024 SAE INTERNATIONAL  
(Further use or distribution is not permitted without permission from SAE.)

## 要旨

自動車向けの排ガス浄化触媒では、活性物質として白金(Pt)・パラジウム(Pd)・ロジウム(Rh)が使われている。このうち、Rhは効率的にNO<sub>x</sub>の還元反応を促進させることができ、必須な元素である。一方、近年ではRhの価格が高騰しており、触媒のコスト増加が問題となっている。希少資源の供給リスクの観点からも、触媒中のRhを代替する、または使用量を削減する技術の開発が急がれる。我々は、(国研)科学技術振興機構のACCELプログラムで開発された“擬ロジウム合金”に注目し、これを用いた触媒の二輪車への適用を検討するとともに、劣化過程の調査を行った。

ナノサイズのPdRuIr合金をセリアジルコニア固溶体へ担持した触媒(PdRuIr/CZ触媒)を作製し、二輪車へ搭載して排ガス計測を行った。担持量4.0g/LのPdRuIr/CZ触媒は0.3g/LのRh/CZ触媒に匹敵する初期特性を有するが、850°C、5hrの熱処理を施すとHC、NO<sub>x</sub>の排出量が増加し、Rh/CZ触媒には劣る結果となった。触媒粉末のX線回折、透過電子顕微鏡観察により、熱処理後には合金粒子の粗大化や相分離が起きていることが確認できた。さらに、評価部品の作製過程でイリジウム(Ir)が酸化していることも確認できた。触媒の作製過程や排ガスに曝される中で、Irが酸化と還元を繰り返しながら相分離が進行していくと推測する。

今回、我々はPdRuIr/CZ触媒の劣化過程を明確にし、Irの酸化が合金の相分離を引き起こす要因であると結論付けた。今後は触媒の耐久性向上、材料費低減を目指し、Irを使わない合金系を探索していく。

## Abstract

Platinum (Pt), palladium (Pd), and rhodium (Rh) are used as active substances in exhaust gas purification catalysts for automobiles. Among these, Rh is an essential element because it efficiently promotes a NO<sub>x</sub> reduction reaction. On the other hand, the price of Rh has been rising in recent years. From the perspective of the supply risk of rare resources, there is an urgent need to develop technologies to replace or reduce the amount of Rh used in catalysts. We focused on the pseudo-rhodium alloy developed by the ACCEL program of the Japan Science and Technology Agency (JST), and then investigated the application of the pseudo-rhodium alloy on the catalysts of our motorcycles and also the degradation process.

A nanosized PdRuIr alloy supported on a ceria-zirconia solid solution (PdRuIr/CZ) was prepared and assembled into a motorcycle for emissions measurement. The PdRuIr/CZ catalyst with an alloy loading of 4.0 g/L had initial properties comparable to the Rh supported on a CZ (Rh/CZ) catalyst with a Rh loading of 0.3 g/L, but after degradation treatment, emissions increased and were inferior to the Rh/CZ. X-ray diffraction and transmission electron microscopy of the catalyst powder showed that the alloy particles increased in size and underwent phase separation after degradation treatment. Furthermore, it was confirmed that iridium (Ir) was oxidized during the specimen preparation process. It is speculated that phase separation proceeds as iridium undergoes repeated oxidation and reduction during the catalyst production process and exposure to exhaust gases.

We have clarified the degradation process of PdRuIr/CZ catalysts and concluded that iridium oxidation is one of the major factors causing phase separation of the alloy.

## 1 INTRODUCTION

The need to address the issue of air pollution to help protect the environment and prevent health hazards has resulted in the introduction of increasingly stringent emissions regulations covering motorcycles. To purify the substances covered in these regulations (carbon monoxide (CO), hydrocarbons (HC), and nitrogen oxides (NOx)), vehicle exhaust systems are equipped with an emissions purification catalyst that uses platinum (Pt), palladium (Pd), and rhodium (Rh) as active substances. Among these, Rh is indispensable since it is the only active substance capable of efficiently promoting NOx reduction reactions. However, faced with rising Rh prices and the supply risks involved in procuring rare resources, there is an urgent need to develop technologies to replace or minimize the amount of Rh used in catalysts. Therefore, this research focused on the pseudo-rhodium alloy<sup>[1]</sup> developed by the ACCEL program of the Japan Science and Technology Agency (JST). This pseudo-rhodium alloy is a nanosized Pd-Ru alloy produced through fusion between Pd and Ru at the atomic level. It features an electron state similar to Rh and reportedly achieves superior NOx purification performance to Rh<sup>[2]</sup>. It has also been reported that adding iridium (Ir) to create a PdRuIr alloy enhances catalytic activity and restricts phase separation under high temperatures<sup>[3]</sup>.

This paper describes the preparation of a PdRuIr/CZ catalyst consisting of a PdRuIr alloy supported on ceria-zirconia (CZ), an evaluation of its emissions purification performance, and an investigation of its degradation process.

## 2 MATERIALS & METHODS

### 2-1. Material Preparation

#### 2-1-1. Alloy Composition Samples

Table 1 describes the samples that were produced to study the optimum alloy composition. These samples were prepared with the cooperation of Kyoto University using a synthesis technique that simultaneously generates the alloy in the liquid phase and sets it on the surface of the CZ support.

Table 1 Alloy composition

	Alloy concentration in powder [wt%]	composition [at%]		
		Pd	Ru	Ir
Sample-1	0.71	10.1	51.2	38.7
Sample-2	0.71	23.3	44.1	32.6
Sample-3	0.79	34.6	36.5	28.9
Sample-4	0.78	43.5	30.7	25.8
Sample-5	0.89	61.7	21.1	17.2

#### 2-1-2. Test Specimens (Emissions Measurement)

The PdRuIr/CZ used for the emissions evaluation was synthesized by Furuya Metal Co., Ltd. using this technique that simultaneously generates the alloy in the liquid phase and sets it on the surface of the CZ support. Table 2 describes the details of the composition. Due to the difficulty of using X-ray diffraction and transmission electron microscopy (TEM) to measure low loading concentrations, the powder was prepared with a high loading concentration of active material. The Rh/CZ powder that was prepared for comparison was synthesized by impregnation using a Rh(NO<sub>3</sub>)<sub>3</sub> solution.

Each powder was dispersed in ion-exchanged water, blended with binder, alumina, CZ, and so on to fabricate the catalyst slurry. The slurry dipping method was adopted to coat the slurry onto the metal honeycomb. The coating amount was then adjusted by air blowing. The test specimens were then produced by forming coating layers in a 1-hour baking process at 450°C in air. For comparison, specimens subjected to degradation treatment were also prepared. Table 3 lists the degradation treatment conditions. The heating furnace temperature was set to achieve a catalyst temperature of approximately 850°C.

A preliminary study was conducted using model gases to estimate the amount of alloy and Rh that would result in similar NOx emissions before degradation treatment. The PdRuIr/CZ catalyst was adjusted to a PdRuIr alloy content of 4.0 g/L. In contrast, the Rh/CZ catalyst was adjusted to an Ru content of 0.3 g/L.

**Table 2 Alloy loading concentration and composition of prototype powders**

Alloy concentration in powder [wt%]	Alloy composition [at%]		
	Pd	Ru	Ir
12.58	21.6	38.2	40.2

**Table 3 Degradation treatment conditions**

temperature	furnace: 805°C specimen: approx. 850°C		
time	5 hours		
gas composition	rich	O <sub>2</sub> : 0.5vol%, CO: 4.0vol%, H <sub>2</sub> O: 10vol%, N <sub>2</sub> : balance	
	lean	O <sub>2</sub> : 5.0vol%, H <sub>2</sub> O: 10vol%, N <sub>2</sub> : balance	
fluctuation pattern	rich gas: 30 sec, lean gas: 10 sec		

## 2-2. Evaluation of Catalytic Activity Using Model Gas

To study the alloy composition, the purification characteristics of the catalysts were evaluated with a model gas using a SIGU-1000 tester manufactured by Horiba, Ltd. The catalyst powder was compacted in a pressing machine and crushed into pellets. These pellets were then sieved into a size between 0.5 and 1 mm and the sample amounts were adjusted to create a PdRuIr alloy weight of 2.8 mg. Table 4 lists the pre-treatment conditions and Table 5 lists the test conditions.

**Table 4 Pre-treatment conditions**

temperature (furnace)	750°C		
time	2 hours		
gas composition	rich	O <sub>2</sub> : 0.5vol%, CO: 4.0vol%, H <sub>2</sub> O: 10vol%, N <sub>2</sub> : balance	
	lean	O <sub>2</sub> : 5.0vol%, H <sub>2</sub> O: 10vol%, N <sub>2</sub> : balance	
fluctuation pattern	rich gas: 30 sec, lean gas: 10 sec		

**Table 5 Test conditions**

temperature (furnace)	start	170°C
	end	600°C
	rate	20°C/min
gas composition	CO <sub>2</sub> : 12.12vol%, O <sub>2</sub> : 0.92vol%, C <sub>3</sub> H <sub>6</sub> : 0.336vol%, C <sub>3</sub> H <sub>8</sub> : 0.084vol%, CO: 0.92vol%, NO: 0.12vol%, H <sub>2</sub> O: 10vol%, N <sub>2</sub> : balance	

## 2-3. Emissions Measurement

The emissions of a motorcycle equipped with a 155 cc liquid-cooled engine that complies with the Euro 4

emissions regulations were measured on a chassis dynamometer (37 kW) manufactured by Ono Sokki Co., Ltd.

- Test cycle: Worldwide Harmonized Motorcycle Emissions Certification Procedure (WMTC) Class 2 Subclass 2-1
- Emissions measurement: MEXA-ONE emissions measurement system manufactured by Horiba, Ltd.

## 2-4. Alloy Composition Analysis

The Pd, Ru, and Ir content of the catalyst powder was measured by high-frequency inductively coupled plasma emission spectrometry. The catalyst powder was dissolved and liquified by the alkali fusion method. A Plasma Quant PQ9000 spectrometer manufactured by Analytik Jena GmbH & Co. was used to measure the content by the calibration curve method.

## 2-5. Specific Surface Area Measurement

The Brunauer-Emmett-Teller (BET) specific surface area was measured using N<sub>2</sub> adsorption to compare the specific surface area of the catalysts before and after the test. This was accomplished by 1-point BET analysis using a Flow Sorb II 2300 apparatus manufactured by Micromeritics Instrument Corp.

## 2-6. Measurement of Quantity of Adsorbed CO

The quantity of adsorbed CO was measured as an indicator of the metal surface area of the catalysts. This was carried out by the CO pulse method using the R-6015H fully automatic catalytic gas absorption measuring apparatus manufactured by HEMMI Slide Rule Co., Ltd. Pretreatment consisted of heat treatment for 15 minutes at 400°C under an O<sub>2</sub> environment, followed by a helium (He) purge and reduction treatment for 15 minutes at 400°C under a hydrogen gas (H<sub>2</sub>) environment.

## 2-7. TEM Observation

A transmission electron microscope (TEM) manufactured by JEOL Ltd. was used to observe and identify the state of the alloy particles supported on the catalysts. The

JEM-F200 multi-purpose electron microscope and JEM-ARM300F2 atomic resolution analytical microscope were used to observe the synthesized catalyst powder. After the degradation treatment, the catalyst powder was observed at an accelerating voltage of 200 kV using a JEM-2100F electron microscope. Elemental analysis was performed using a JED-2300 energy dispersive X-ray spectrometer (EDX).

### 2-8. X-Ray Diffraction (XRD) Measurement

The crystalline structure and composition of the alloy particles were verified by XRD measurement using an X’Pert PRO MPD X-ray diffractometer manufactured by Spectris. Copper (Cu) tubes were used as the X-ray source and CuK $\alpha$  rays were used as a probe X-rays.

## 3 RESULTS

### 3-1. Alloy Composition Study

Five samples were fabricated to evaluate the different purification characteristics of the alloy compositions. Figures 1 to 3 show the evaluation results. Sample 2 demonstrated the highest low-temperature activity for the purification performance of CO, HC, and NO. Sample 2 was fabricated with a Pd:Ru:Ir alloy composition of 2:4:4. In response, an alloy-loaded powder with the same composition was produced for emissions measurement using an actual motorcycle.

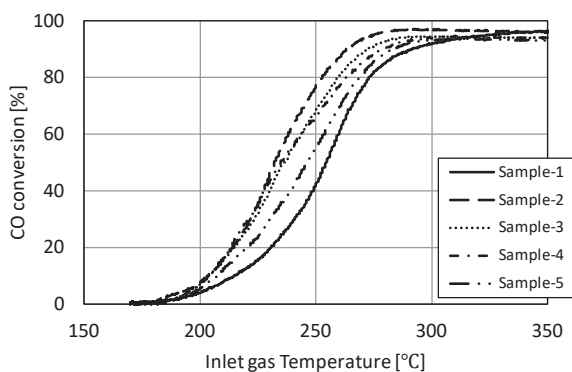


Fig. 1 CO purification characteristics using model gas

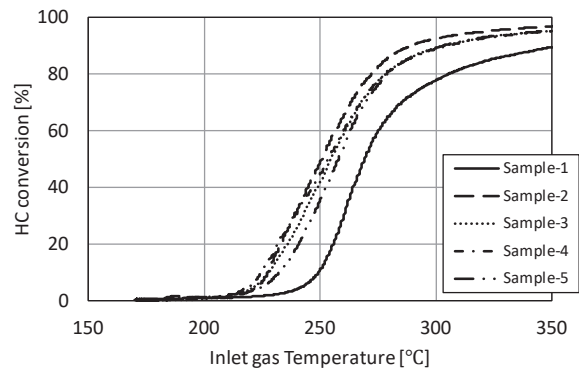


Fig. 2 HC purification characteristics using model gas

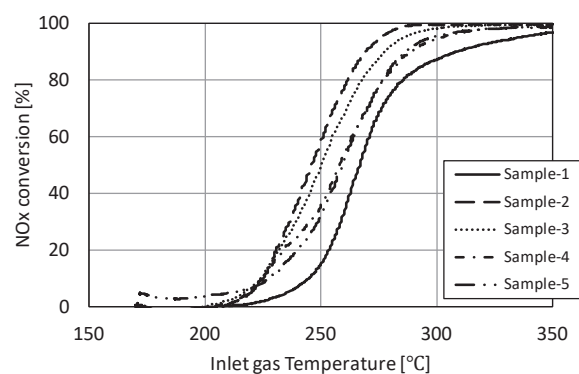


Fig. 3 NOx purification characteristics using model gas

### 3-2. Emissions Measurement

Figure 4 shows the emissions measurement results using motorcycles equipped with PdRuIr/CZ catalysts. Before the degradation treatment, the total hydrocarbon (THC) emissions were higher than the Rh/CZ catalyst. However, the CO and NOx emissions were the same, confirming the excellent NOx purification characteristics of a catalyst with this alloy composition. However, emissions increased after the degradation treatment and were substantially worse than the Rh/CZ catalyst, highlighting the fact that durability will be an issue for practical adoption.

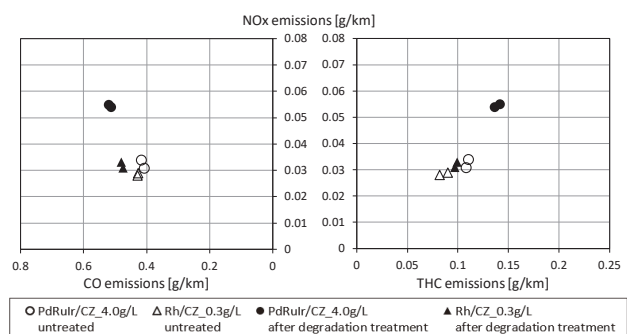


Fig. 4 Emissions measurement results after test cycle

### 3-3. Investigation of Degradation State

The degradation state was investigated to help improve the durability of the PdRuIr/CZ catalyst. It is known that both Ru and Ir oxidize under high-temperature oxidizing conditions and evaporate into a gaseous phase. Since the active material of this catalyst consists of nanoparticles, this oxidation and evaporation process might occur at lower temperatures. Therefore, once emissions measurement was completed, catalyst powder was extracted from the test specimens after the degradation treatment, and the Pd, Ru, and Ir content was analyzed (Fig. 5). The extracted powder was compared with fresh powder obtained by drying the catalyst slurry. No changes in the element content were identified after the degradation treatment, indicating that evaporation of Ru or Ir had not occurred.

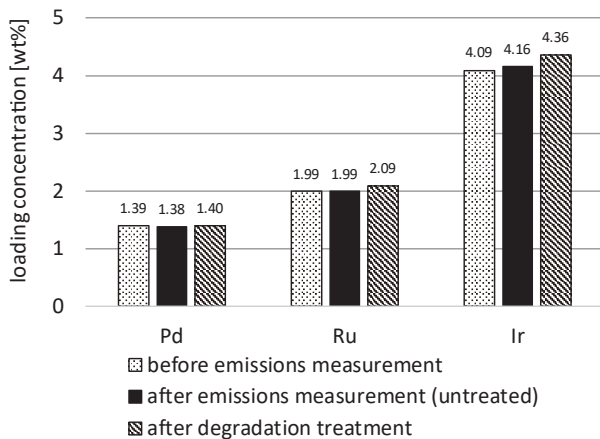


Fig. 5 Results of element content analysis

Figure 6 shows the CZ specific surface area measurement results. These results indicate that the specific surface area fell due to the heat load applied by the emissions measurement and degradation treatment, and that the CZ particles increased in size. However, the specific surface area of CZ that is not loaded with alloy falls only slightly after heat treatment for 5 hours at 850°C in air. Therefore, this drop in specific surface area seems to be a particular phenomenon caused by the loading of the alloy onto the CZ.

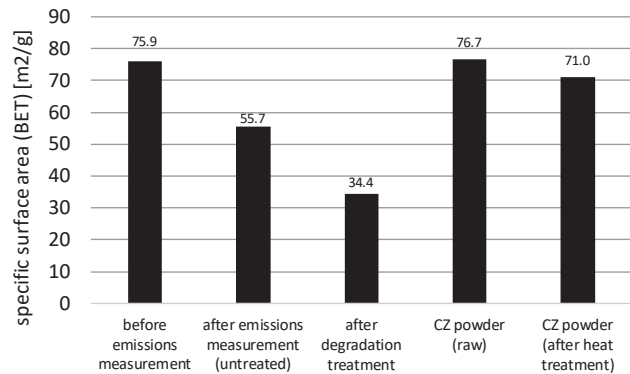


Fig. 6 Specific surface area trend

It was estimated that the increase in the size of the support particles caused the PdRuIr alloy particles on the surface of the CZ to coalesce or sink into the support, resulting in a lower alloy surface area. Subsequently, the quantity of adsorbed CO was measured as an indicator of the alloy surface area (Fig. 7). The quantity of adsorbed CO fell in the same way as the specific surface area of the support, also indicating that the alloy surface area decreased in size. Next, the alloy particles were observed using TEM. Figure 8 shows observation images of the catalyst powder after PdRuIr alloy loading and Fig. 9 shows element map images. These images show that, immediately after alloy loading, a PdRuIr alloy with a particle size of several nm was produced. Visual field 1 in Fig. 8 shows a location at which the alloy particles have aggregated, whereas visual field 2 shows that this location also contains areas in which the alloy loading state is comparatively dispersed. Figure 10 shows the catalyst powder after degradation treatment. In these images, particles sized between 10 and 100 nm can be observed. In addition, superimposed elemental analysis images show that the composition inside the particles is not uniform and that phase separation has probably occurred inside the particles.

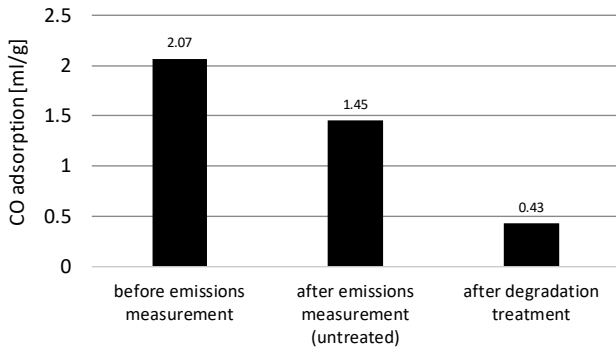
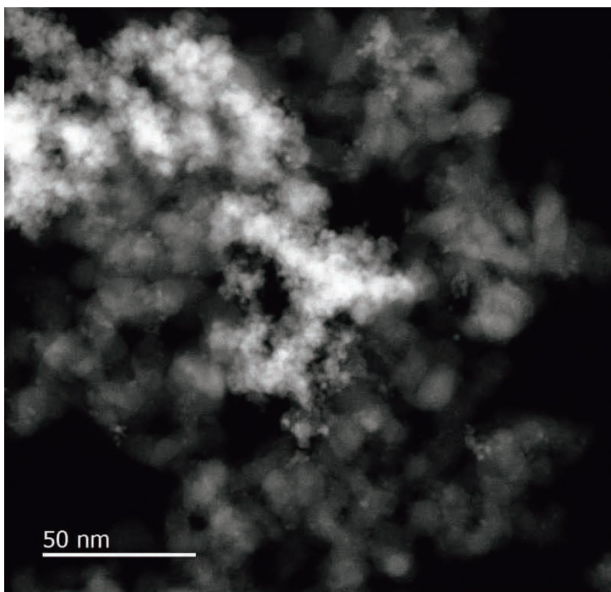
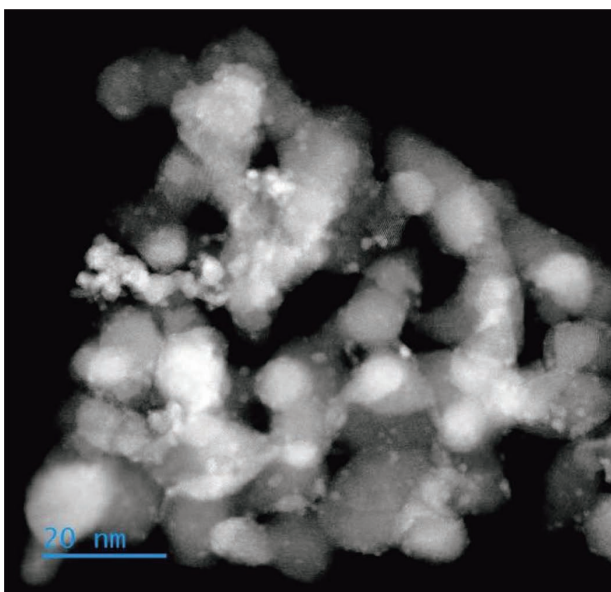


Fig. 7 CO adsorption trend



Visual field 1 (JEM-F200)



Visual field 2 (JEM-ARM300F20)

Fig. 8 Appearance of catalyst powder after PdRuIr alloy loading

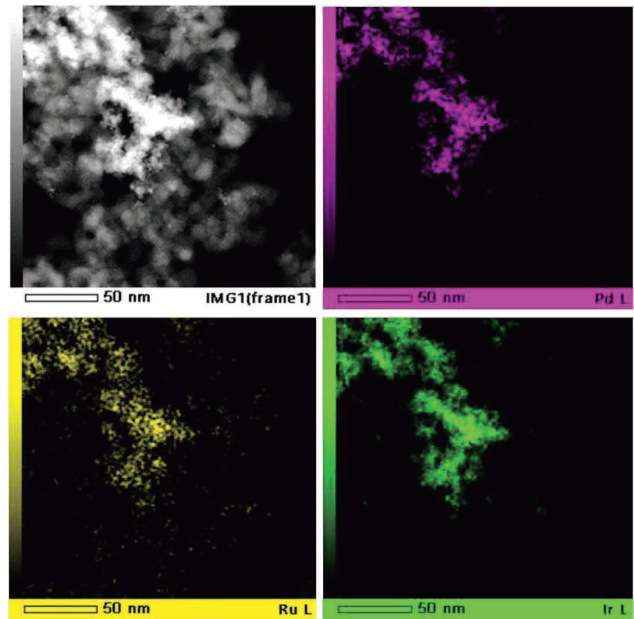


Fig. 9 Element map of catalyst powder after synthesis (visual field 1 in Fig. 8)

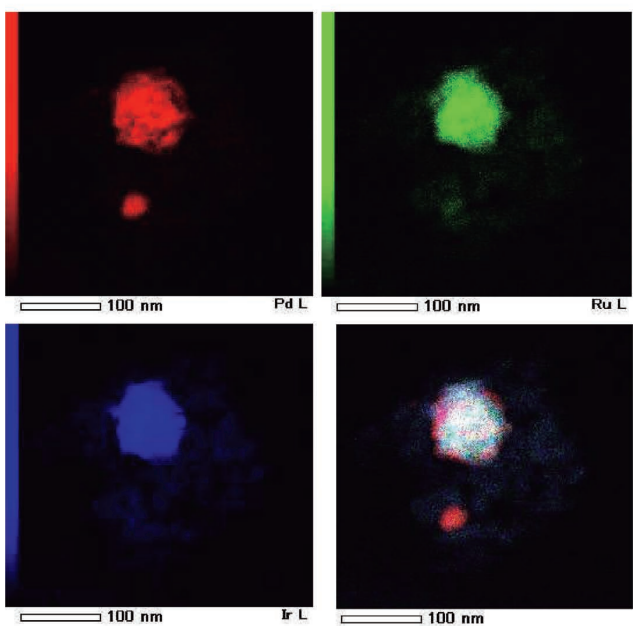
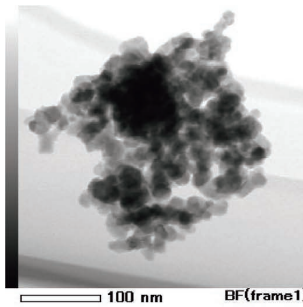


Fig. 10 Element map of alloy particles after degradation treatment

The phase separation process of the alloy particles was investigated by XRD. Figure 11 shows the XRD pattern. Data item 3 shows the diffraction pattern immediately after PdRuIr alloy loading. In addition to the CZ-derived peak, a broad peak around 40.7° is also present. In results measured by Kusada et al.<sup>[3]</sup> using synchrotron radiation ( $\lambda = 0.578980 \text{ \AA}$ ), the (111) phase of PdRuIr was observed close to  $2\theta = 15^\circ$ ). When the results measured by Kusada et al. were converted to the wavelength of the CuK $\alpha$  rays ( $\lambda = 1.54060 \text{ \AA}$ ) used in this research, the peak around 40.7° corresponds with the (111) phase of PdRuIr. The synthesis of nanosized PdRuIr alloy can also be recognized from the X-ray diffraction pattern. Data item 4 is the catalyst powder after a 1-hour baking process at 450°C in air during the process to fabricate the specimens for emissions evaluation. The diffraction peak derived from PdRuIr disappears and a peak derived from IrO<sub>2</sub> appears. This result suggests that the Ir in the alloy was oxidized by the baking process, causing the PdRuIr alloy state to break down. In contrast, after emissions measurement (data item 5) and degradation treatment (data item 6), the diffraction peak around 40.7° appears again. At the same time, peaks derived from IrRu and IrPd also appeared, creating a mixed condition of PdRuIr, IrRu, and IrPd. This is considered to be the state inside the particles shown in Fig. 10.

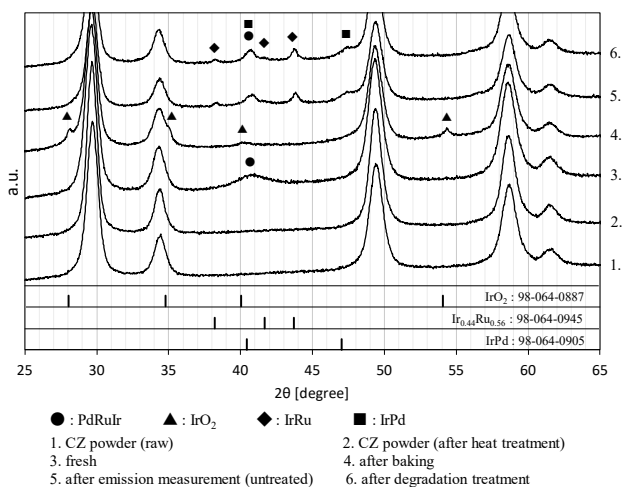


Fig. 11 X-ray diffraction pattern of catalyst powder (reference data: only peaks with an intensity ratio of 20% or higher are shown)

## 4 DISCUSSION

Based on the analysis results described above, the emissions purification characteristics of the PdRuIr/CZ catalyst fell due to enlargement of the CZ and alloy particles and phase separation of the alloy. The aim is to address these issues and realize practical adoption of a pseudo-rhodium alloy catalyst.

Loading the PdRuIr alloy onto the CZ support seems to facilitate a decrease in the CZ specific surface area. One possible cause of this issue is the formation of a Ru and Ir solid solution. Since oxides of Ru and Ir have a lower melting temperature than CZ, these oxides might act as sintering aids. Another possible cause is hydrothermal degradation or the like in the alloy synthesis process. Continued efforts are required to identify the causes and study countermeasures.

One of the main causes of alloy particle phase separation is thought to be changes in the crystalline structure due to the oxidation and reduction of Ir. The results of this investigation found that IrO<sub>2</sub> was being generated easily at a relatively low temperature of 450°C. The catalyst is exposed to higher temperature oxidizing and reduction conditions under the actual exhaust gas environment generated during riding and the degradation treatment conditions of this test. The crystalline structure of Ir undergoes major changes when it transforms to and from its oxide and metal states. These changes probably facilitate its transition to more stable IrRu and IrPd phases. It may be possible to suppress this phase separation by adopting an element that is less susceptible to oxidation than Ir, such as Pt. As Ir becomes more expensive, the switch to a lower cost element would also be a rational measure in some terms. Studies will be continued.

## 5 CONCLUSIONS

This paper studied the optimum composition for a PdRuIr alloy and evaluated the performance of a PdRuIr/CZ catalyst on an actual motorcycle. Although the test

confirmed that this catalyst has an excellent NO<sub>x</sub> conversion capacity, it also identified an issue related to durability. The results verified that catalyst degradation was caused by enlargement of the CZ and alloy particles and phase separation of the alloy. One of the main cause of this phase separation is thought to be Ir oxidation.

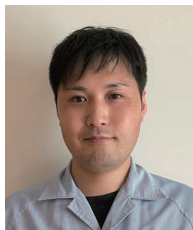
### ACKNOWLEDGMENTS

The authors would like to express their sincere gratitude to everyone involved in this research, notably Professors Hiroshi Kitagawa and Kohei Kusada of Kyoto University, as well as Kyoto University, Furuya Metal Co., Ltd., and Sakura Kogyo Co., Ltd. for their invaluable cooperation in the manufacture and material analysis of the alloy support powder, and in carrying out the emissions measurement.

### REFERENCES

- [1] Kusada, K., Kobayashi, H., Ikeda, R., Kubota, Y. et al. “Solid Solution Alloy Nanoparticles of Immiscible Pd and Ru Elements Neighboring on Rh: Changeover of the Thermodynamic Behavior for Hydrogen Storage and Enhanced CO-Oxidizing Ability”, *J. Am. Chem. Soc.*, 136, 1864, (2014). doi: 10.1021/ja409464g.
- [2] Sato, K., Tomonaga, H., Yamamoto, T., Matsumura, S. et al. “A Synthetic Pseudo-Rh: NO<sub>x</sub> Reduction Activity and Electronic Structure of Pd-Ru Solid-solution Alloy Nanoparticles”, *Sci. Rep.*, 6, 28265, (2016). doi: 10.1038/srep28265.
- [3] Kusada, K., Wu, D., Nanba, Y., Koyama, M. et al. “Highly Stable and Active Solid-Solution-Alloy Three-Way Catalyst by Utilizing Configurational-Entropy Effect”, *Advanced Materials*, 33, 2005206, (2021). doi: 10.1002/adma.202005206.

### ■ 著者



茂木 卓也  
Takuya Motegi  
生産技術本部  
材料技術部



多々良 俊哉  
Shunya Tataka  
生産技術本部  
材料技術部



高本 駿平  
Shunpei Takamoto  
生産技術本部  
材料技術部



土居 航介  
Kosuke Doi  
生産技術本部  
材料技術部